

Absolute dating of brittle fault movements: Late Permian and late Jurassic extensional fault breccias in western Norway

Elizabeth A. Eide^{1*}, Trond H. Torsvik^{1,2} and Torgeir B. Andersen³

¹Geological Survey of Norway, PO Box 3006 Lade, N-7002 Trondheim, Norway, ²Department of Solid Earth Physics, University of Bergen, N-5002 Bergen, Norway, ³Department of Geology, University of Oslo, PO Box 1047 Blindern, 0316 Oslo, Norway

ABSTRACT

⁴⁰Ar/³⁹Ar geochronological and palaeomagnetic dating methods applied to fault breccias in western Norway have isolated two brittle reactivation episodes of the syn-post-Caledonian, extensional Nordfjord-Sogn Detachment. These events, of latest Permian and latest Jurassic–Early Cretaceous ages, demonstrate temporal relationships between development of chemical remanent magnetism and partial resetting of Ar isotopic systems during distinct breccia-forming episodes. A third event of Carboniferous age was also identified in the

breccias with the ⁴⁰Ar/³⁹Ar technique and is a relict unroofing signature inherited from the fault wall-rocks. These brittle faults are significant time markers and become relevant to interpretations of offshore seismic data which attempt to place ages on faults that have undergone multiple reactivation episodes.

Terra Nova, 9, 135–139, 1997

Introduction

The potential of fault rocks to delimit the timing of tectonic events has advanced significantly since the quintessential fault-rock classification schemes of Sibson (1977) and Wise *et al.* (1984). Various isotopic dating methods can be applied to fault rocks to generate absolute ages of fault genesis and have been used with some success on mylonitic rocks in ductile fault zones (Lee, 1991; House and Hodges, 1994) as well as on pseudotachylites (Kelley *et al.*, 1994). Brittle fault rocks, because of their low-temperature nature and associated, ‘open system’ behaviour, are probably more difficult to date accurately with isotopic methods (Gibbons *et al.*, 1996).

We have utilized two different dating techniques to constrain the ages of fault breccia genesis in a reactivated detachment zone in western Norway (Fig. 1). Brittle fault breccias are viable materials for palaeomagnetic determination of the age of a fault-rock matrix that acquired a low-temperature, chemical remanent magnetic (CRM) signature, or the age of breccia clasts from fault wall-rocks that have acquired a partial thermochemical remanent magnetic (TRM) resetting signature (Fig. 2). We have addressed the hypothesis that, with control provided by palaeomagnetic and regional geological data, the ⁴⁰Ar/³⁹Ar geochronological method can accurately identify ages of fault

brecciation in this multiply reactivated fault zone.

The circumstances for dating these brittle fault rocks were ideal as we had excellent tectonostratigraphic control (Osmundsen and Andersen, 1994; Brekke and Solberg, 1987), a shallowly dipping fault breccia, clear cross-cutting relationships between the breccia and the extensional detachment, and K-feldspar-bearing units in both hanging wall and footwall. The rocks were previously dated palaeomagnetically (Torsvik *et al.*, 1992), but the relatively large uncertainties associated palaeomagnetic ages (*c.* ± 10 Myr) encouraged us to reanalyse this earlier dataset

and apply an independent dating technique (⁴⁰Ar/³⁹Ar) to the same rocks. The data illustrate complementary and supplementary powers of the two techniques when utilized in well-documented tectonostratigraphic settings.

Geological background

The Caledonian history of western Norway involved arc- and continental-collision and high-ultrahigh-pressure (HP-UHP) metamorphism as Baltic crust subducted beneath Laurentia from ≈ 450–410 Ma (Cuthbert *et al.*, 1983; Smith, 1984; Eide and Torsvik,

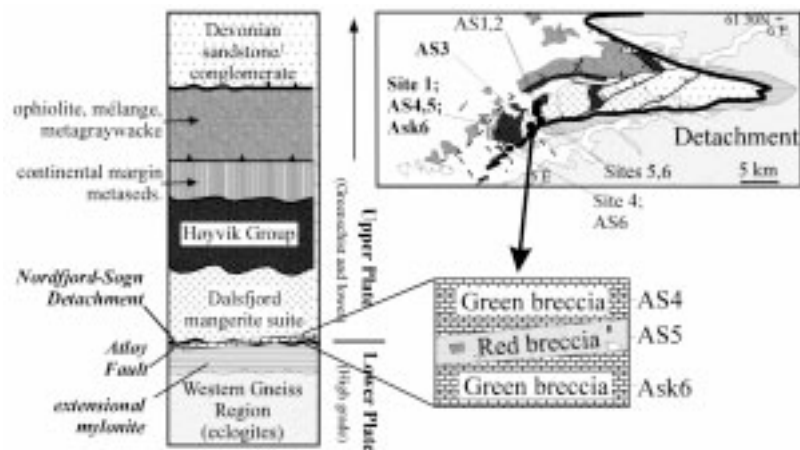


Fig. 1 Geological map and tectonostratigraphic column, modified after Osmundsen and Andersen (1994), showing relationships around the Nordfjord-Sogn Detachment (NSD) zone. High grade, eclogite-bearing basement of the Western Gneiss Region is overlain by weakly metamorphosed, allochthonous units with broadly Ordovician, white-mica cooling ages. On Atføy, the NSD was cut by two different brittle faults. Sample sites include those for ⁴⁰Ar/³⁹Ar dating (‘AS’ prefixes) and from the palaeomagnetic study of Torsvik *et al.* (1992) (‘Site’ prefixes).

Correspondence: Tel: + 47/73 90 4237; Fax: + 47/73 92 1620; E-mail: elizabeth.eide@ngu.no

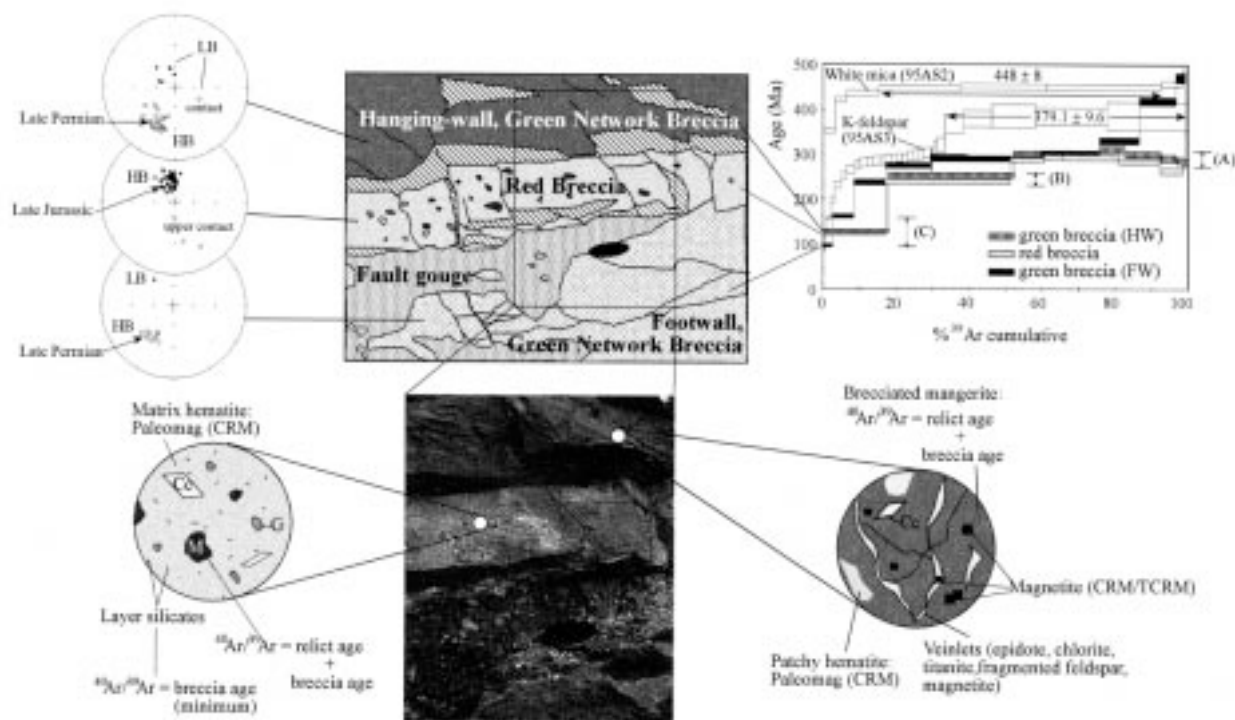


Fig. 2 Photograph and line drawing of the Atløy red and green fault breccias. Lower figure: application of the palaeomagnetic and $^{40}\text{Ar}/^{39}\text{Ar}$ dating techniques to fault rocks. Top left: HB and LB palaeomagnetic components from the three breccias. Note the dual polarity nature of the HB component in the red breccia. Top right: release spectra for the red and green breccias, a cycled, isothermal heating experiment from a mangerite feldspar, and white mica from the Upper Plate (see also Fig. 1). Age ranges (A), (B) and (C) correspond to separate thermochemical events (see text for details).

1996). Exhumation of deeply buried rocks by extensional collapse was accommodated by vertical shortening/horizontal stretching of the lower crust and large-scale, normal movement on a system of extensional detachments (Andersen and Jamtveit, 1990; Andersen *et al.*, 1991, 1994). Extensional shearing along the main Nordfjord–Sogn Detachment (NSD) is manifested as 2–3 km-thick extensional mylonites that juxtapose ‘Lower Plate’, eclogitic basement and ‘Upper Plate’, allochthonous rocks plus Devonian sedimentary basins (Fig. 1).

The NSD and extensional mylonite are folded (Roberts, 1983) and intersected by brittle faults, the most spectacular of which outcrops on the island of Atløy where a nearly flat-lying, fault-breccia zone cuts the NSD (Figs 1 and 2). The fault-breccia zone comprises a green network breccia and a cross-cutting red breccia. The latter is a 15–35 cm-thick package dipping $\approx 10^\circ$ W and separates hanging wall (HW) from footwall (FW) green network breccias (Fig. 2) (Brekke and Solberg, 1987; Torsvik *et al.*, 1992). The HW green

breccia reworked rocks of the Upper Plate Dalsfjord mangerite suite while the FW green breccia reworked both Upper Plate rocks and Lower Plate mylonites.

The nonbrecciated, Upper Plate, Dalsfjord mangerite-syenite contains micropertthitic alkali feldspar, white mica, titanite, epidote, magnetite and ilmenite, orthopyroxene altered to chlorite, and minor calcite. The HW, green breccia comprises subangular feldspar clasts surrounded by veinlets with fine, feldspar fragments, chlorite, epidote, titanite, magnetite and fine, layer silicates (Fig. 2). The large clasts have subgrains and partially annealed fractures. The FW and HW green breccia are similar.

The red breccia comprises angular, mm- to cm-sized clasts in a fine-grained, brick-red matrix (Fig. 2). Rock clasts comprise greenish network-breccia fragments, calcite, minor layer silicates and oxides. Feldspar clasts occur either as masses of very fine, equigranular subgrains or coarse, twinned subgrain clusters, reminiscent of green-breccia clasts.

Summary of palaeomagnetic data

The magnetic mineralogies of both HW and FW green breccias comprise mainly magnetite, with accessory haematite and pyrrhotite. The FW breccia is dominated by high-temperature (HT) components with SSW declinations and negative inclinations (Fig. 2). This HT component, assigned a Late Permian age (250 Myr) by Torsvik *et al.* (1992), is sporadically overprinted by a younger, low-blocking (LB) component with NNW declinations and steep positive inclinations; the LB overprints are more pronounced in the HW than in the FW green breccia.

The red-breccia fabric is almost isotropic and has a haematite- and goethite-stained matrix with abundant pyrrhotite and accessory magnetite. NNW declinations with steep positive inclinations prevail (Fig. 2), but along the upper contact of the red breccia we notice a polarity shift; hence, cementation and fluid fluxes in the red breccia appear to cover a reversal of the Earth’s magnetic field. The same LB (dual-polarity) component identified in the

green breccias is the principal high-blocking (HB) magnetization component in the younger red breccia; this HB component (Fig. 2) was assigned a late Jurassic–Early Cretaceous age (150 Myr) (Torsvik *et al.*, 1992). The stronger influence of LB components in the HW green breccia vs. the FW green breccia is attributed to expulsion of red-breccia fluids into the HW; the fluid infiltration is observed now as red patches in the upper green breccia close to the red-breccia contact. Analytical details, magnetic mineralogy and strain fabrics related to these palaeomagnetic data are presented in Torsvik *et al.* (1992).

$^{40}\text{Ar}/^{39}\text{Ar}$ data

We used furnace step-heating to analyse a red-breccia whole rock, HW and FW green-breccia whole rocks, K-feldspar clasts separated from the HW breccia, and white mica and K-feldspar separates from several Upper and Lower Plate units (Figs 1 and 2). Analyses were conducted at the Laboratoire de Géologie, Université Blaise Pascal et CNRS, Clermont-Ferrand, France with a protocol similar to Arnaud *et al.* (1993). Results and discussion of isothermal, cycled heating experiments and diffusion modelling of the K-feldspars will be presented elsewhere (Eide *et al.* in prep.). Ages are cited at the 1σ confidence interval, with J -value error. Complete data tables are available from the authors.

Whole-rock fault-breccia data

The first two steps of the HW green-breccia spectrum comprise 52.2% of total $^{39}\text{Ar}_K$ gas and yield apparent ages of 129.5 ± 2.7 Myr and 253.2 ± 4.6 Myr, respectively (Fig. 2). The latter half of the spectrum gives a slightly disturbed group of semiconcordant steps with a weighted age of 296.2 ± 2.6 Ma (8 steps). Eleven steps from the FW green breccia define a pattern of ages which climb rapidly from 96.4 ± 2.5 Myr to a group of semiconcordant steps (steps 4 through 7; 58.4% of total $^{39}\text{Ar}_K$ gas) with a weighted age of 296.4 ± 2.8 Myr. Ages in the final 25% of the FW breccia spectrum climb rapidly to unrealistically high values (Fig. 2). The red-breccia release spectrum is identical to that of the HW green breccia and is characterized by

an imprecise age of 286.6 ± 3.3 Myr in the upper temperature portion of the experiment (48.6% of gas, excluding the last step which comprised only air) and significantly younger first and second steps (122.2 ± 3.0 Myr and 238.3 ± 5.7 Myr) (Fig. 2).

The K/Ca ratios for the green HW and red breccias are similarly characterized by high initial values that drop and then climb in the higher-temperature portions of the experiments. K/Ca values drop again as the samples approach fusion (Fig. 3). The FW breccia exhibits a broadly similar pattern in the high-temperature, high-age steps, with a slightly lower initial K/Ca ratio compared to the other breccias. The Cl/K ratios for all three breccias are fairly low and exhibit a gradual increase through the high-age, high-temperature steps (Fig. 3).

Inverse isochron analysis of the red and HW green breccia data was not useful due to their highly radiogenic nature. Isochron analysis of the FW green breccia data clearly indicates excess Ar in the final four, high-temperature steps that yielded anomalously high ages.

White mica and K-feldspar

The spectrum for white mica from the Upper Plate Høyvik Group, overlying the mangerite, gives a plateau age of 448 ± 8 Myr (77% of $^{39}\text{Ar}_K$ released; sample AS2; Figs 1 and 2; Eide *et al.*, 1996). This age is within uncertainty of cooling ages from the same unit on Atløy and several other Upper Plate white micas (Andersen *et al.*, in press).

The spectra from isothermal, cycled heating experiments of K-feldspar separates from Upper and Lower Plate

rocks (AS1, AS2, AS3, and AS6; Fig. 1) have identical release patterns, albeit with some intersample age differences related to partial, Late Permian resetting (Eide *et al.*, 1996; Eide *et al.* in prep.). An example spectrum (AS3), from immediately above the Atløy Fault defines three domains: a low-temperature domain of rapidly climbing ages (86.5–265.9 Myr), an intermediate-retentivity domain of semi-concordant-to-slightly increasing steps (292.6 ± 2.3 Myr, weighted age), and a high-temperature domain of concordant steps (379.1 ± 9.6 Myr, weighted age) (Fig. 2).

Discussion of $^{40}\text{Ar}/^{39}\text{Ar}$ data

The whole-rock spectra define three different age groups (ranges A, B and C, Fig. 2) corresponding to separate thermal episodes. Large volumes of Ar gas released in the whole-rock experiments resided in the K-feldspar clasts and distinguished inherited (relict, wall-rock) and new (brecciation-related) ages. Age range (A) (from ≈ 287 and 310 Ma) comprises the central group of semiconcordant ages in the FW breccia, the highest temperature portions of the HW green and red breccia spectra, and the intermediate domain in the K-feldspar (AS3). Age range (B) (from 238 to 253 Ma) represents a *minimum* resetting age and incorporates the second step in each of the red and HW green breccias, the concordant step from the FW breccia, and the downward cusp in the K-feldspar spectrum. Age range (C) (from 96 to 162 Ma) represents a *maximum* age range for the youngest resetting episode(s).

These three age groups document resetting of < 300 Myr old rocks (inherited age A) during one pervasive event older than 253 ± 5 Myr (the maximum of range B, Fig. 2). A less thorough resetting event, or events, occurred in sub-late-Jurassic times (range C, Fig. 2). The ages within (C) are indicative of partial Ar loss during at least two events: one more recent than 96 ± 3 Ma (perhaps associated with genesis of clay-rich fault gouge; see Fig. 2) and one event at least younger than 238 Ma and, most likely, younger than 163 ± 4 Ma (the maximum limit of range C). The latter event can be linked to the younger of two palaeomagnetic ages and probably dates the genesis of the red breccia (see 'Data comparison').

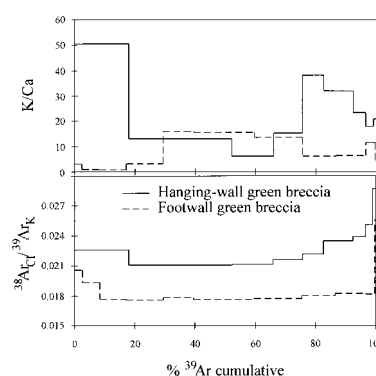
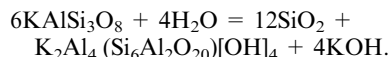


Fig. 3 K/Ca and $^{38}\text{Ar}_{Cl}/^{39}\text{Ar}_K$ ratios for whole-rock samples.

The higher, relative initial K/Ca ratios and low apparent ages in the first step of each whole-rock spectrum are attributable to outgassing of high-K phases with low Ar retentivity (Figs 2 and 3). The likely sources are fine-grained layer silicates in the rock matrices and low-retentivity, fine-grained portions of the K-feldspar clasts with some Cl-contribution from matrix chlorite. Genesis of the low-temperature layer silicates is linked to partial replacement of K-feldspar breccia clasts by quartz via the reaction:



Thermal and diffusion modelling of the cycled, isothermal K-feldspar heating experiments from Upper and Lower Plates suggests that the Late Carboniferous age ($\approx 287\text{--}310$ Ma) of range (B) represents partial resetting of an early Carboniferous (350 Ma), rapid cooling event (Eide *et al.*, 1996). The high-retentivity portion (≈ 379 Ma) of the single-grain, K-feldspar experiment (Fig. 2) is neither present in the whole-rock experimental data nor in an analysed separate of K-feldspar HW clasts; the HT feldspar domain was destroyed during younger, grain-size reduction/brecciation events.

Data comparison and synopsis

Figure 4 synthesizes the $^{40}\text{Ar}/^{39}\text{Ar}$ and palaeomagnetic fault-rock ages in the context of an annotated Mid-Palaeozoic to Cretaceous apparent polar wander path (APWP) for Baltica/Europe. Group (B), whole-rock $^{40}\text{Ar}/^{39}\text{Ar}$ ages corroborate Late Permian, green-breccia palaeomagnetic ages of Torsvik *et al.* (1992) and fit closely to the APWP age of 260 Myr. The Late Permian palaeomagnetic age is interpreted as the time of CRM remanence acquisition during green-breccia formation at temperatures < 250 °C (Torsvik *et al.*, 1992) (Figs 2 and 4); the group (B) $^{40}\text{Ar}/^{39}\text{Ar}$ data document a strong resetting event older than 253 ± 5 Ma. The green-breccia forming event is thus constrained between ≈ 248 and 260 Ma. Regionally, extension-related dykes in western and southwestern Norway overlap in time with green breccia formation (Fig. 4; see also Torsvik *et al.*, in press).

Similarly, the palaeomagnetic data from the red breccia fall near the 98–144 Ma pole for Europe and overlap

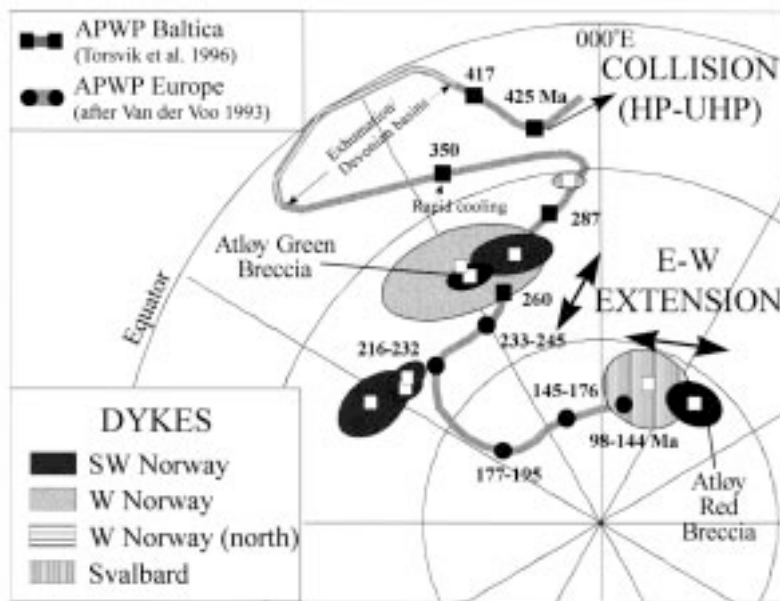


Fig. 4 Synopsis of palaeomagnetic and $^{40}\text{Ar}/^{39}\text{Ar}$ data on an annotated APWP for Baltica/Europe. Dark squares and circles on the APWP and adjacent numbers correspond to pole ages in Myr (after Torsvik *et al.*, 1996 and Van der Voo, 1993).

with data from extension-related dykes (Hinlopen) from Svalbard (Fig. 4). Torsvik *et al.* (1992) suggested the red-breccia data documented genesis of a late Jurassic, HB component, related to CRM acquisition during low-temperature haematite precipitation and red-breccia formation. Confidence in the red-breccia palaeomagnetic pole position is imparted by the dual-polarity nature of the HB component in the rock (LB component in the green breccia). The Group (C), whole-rock $^{40}\text{Ar}/^{39}\text{Ar}$ data constrain red-breccia genesis to be more recent than 162 Ma, with unique definition of the red-brecciation phase complicated by fault-gouge genesis after 96 Ma. The late Jurassic–Early Cretaceous age for red-breccia formation is likewise coincident with regional rifting and basin formation in the northern North Sea (Torsvik *et al.*, 1992; Færseth, 1996).

The fact that the HB component is only weakly developed in the HW green breccia (extracted as the LB component from the rock; see Fig. 2), and is nearly undeveloped in the FW green breccia, is due to the nearly horizontal orientation of the Dalsfjord Fault: warm fluids flowing through a fracture with this orientation would probably have percolated preferentially upwards, leaving very little haematite precipitate in the FW breccia. This implies that the Dalsfjord Fault orientation has not

changed (rotated) significantly since the Early Cretaceous and again, reinforces the position of the red-breccia pole in Fig. 4.

Of the two brittle faulting events, the latest Permian, green-breccia-forming episode was dominant. The magnetic component is unblocked only at high temperatures in both HW and FWs, and the most dramatic impact on the Ar-systematics of the whole-rock systems was effected during the green-brecciation activity. The magnitude of this latest Permian event takes on regional significance not only from broad inferences to early rifting events along the Baltica–Laurentia suture (e.g. Færseth, 1996), but even more directly from the numerous Late Permian mafic dykes exposed along the coast of western Norway (Fig. 4; Torsvik *et al.*, in press).

The common denominator in the brittle fault activity was infiltration of low-temperature fluids and cataclastic activity, manifested both as CRM signatures and Ar-resetting ages. We cannot state with absolute certainty that the Ar ages accurately date the time of CRM acquisition, given the fact that these two age-dating techniques are dependent upon very different properties of mineral systems; however, we emphasize that the palaeomagnetic and Ar data are remarkably consistent with one another and also with constraints provided by regional geology.

Acknowledgements

The authors thank Nicolas O. Arnaud for a very thorough review of an early version of the manuscript and two anonymous reviewers for useful comments. Research was supported by cooperative Mobil-Phillips-Statoil-NGU-NFR project funding to the authors and by a Nansen Fund grant and U.S.-Norway Fulbright Fellowship to EAE. This constitutes ONOFF contribution no. 2.

References

- Andersen, T.B., Berry IV, H.N., Lux, D.R. and Andresen, A., 1997. The tectonic significance of pre-Scandian $^{40}\text{Ar}/^{39}\text{Ar}$ phengite cooling ages in the Caledonides of Western Norway. *J. Geol. Soc. London*, in press
- Andersen, T.B. and Jamtveit, B., 1990. Uplift of deep crust during orogenic extensional collapse: A model based on field studies in the Sogn-Sunnfjord region of Western Norway. *Tectonics*, **9**, 1097–1111.
- Andersen, T.B., Jamtveit, B., Dewey, J.F. and Swenson, E., 1991. Subduction and exhumation of continental crust: major mechanisms during continent-continent collision and orogenic extensional collapse, a model based on the south Norwegian Caledonides. *Terra Nova*, **3**, 303–310.
- Andersen, T.B., Osmundsen, P.T. and Jolivet, L., 1994. Deep crustal fabrics and a model for the extensional collapse of the Southwest Norwegian Caledonides. *J. Struct. Geol.*, **16**, 1191–1203.
- Arnaud, N.O., Brunel, M., Cantagrel, J.M. and Tapponier, P., 1993. High cooling and denudation rates at Kongur Shan, eastern Pamir (Xinjiang, China) revealed by $^{40}\text{Ar}/^{39}\text{Ar}$ alkali feldspar thermochronology. *Tectonics*, **12**, 1335–1346.
- Brekke, H. and Solberg, P.O., 1987. The geology of Atløy, Sunnfjord, western Norway. *Nor. Geol. U. Bull.*, **410**, 73–94.
- Cuthbert, S.J., Harvey, M.A. and Carswell, D.A., 1983. A tectonic model for the metamorphic evolution of the Basal Gneiss Complex, Western South Norway. *J. Metamorph. Geol.*, **1**, 63–90.
- Eide, E.A. and Torsvik, T.H., 1996. Palaeozoic supercontinental assembly, mantle flushing, and genesis of the Kiaman Superchron. *Earth Planet. Sci. Lett.*, **144**, 389–402.
- Eide, E.A., Torsvik, T.H. and Andersen, T.B., 1996. Precise timing of multiple reactivation events on a Caledonian extensional detachment, Western Norway: What happens after exhumation? (abs.). *EOS, Trans. Am. Geophys. Un.*, **77**(46), F779.
- Færseth, R.B., 1996. Interaction of Permo-Triassic and Jurassic extensional fault-blocks during the development of the northern North Sea. *J. Geol. Soc. London*, **153**, 931–944.
- Gibbons, W., Doig, R., Gordon, T., Murphy, B., Reynolds, P. and White, J.C., 1996. Mylonite to megabreccia: Tracking fault events within a transcurrent terrane boundary in Nova Scotia, Canada. *Geology*, **24**, 411–414.
- House, M.A. and Hodges, K.V., 1994. Limits on the tectonic significance of rapid cooling events in extensional settings: Insights from the Bitterroot metamorphic core complex, Idaho-Montana. *Geology*, **22**, 1007–1010.
- Kelley, S.P., Reddy, S.M. and Maddock, R., 1994. Laser-probe $^{40}\text{Ar}/^{39}\text{Ar}$ investigation of a pseudotachylyte and its host rock from the Outer Isles thrust, Scotland. *Geology*, **22**, 443–446.
- Lee, J., 1991. Incremental $^{40}\text{Ar}/^{39}\text{Ar}$ thermochronology of mylonitic rocks from the northern Snake Range, Nevada. *Tectonics*, **10**, 77–100.
- Osmundsen, P.T. and Andersen, T.B., 1994. Caledonian compressional and late-orogenic extensional deformation in the Staveneset area, Sunnfjord, Western Norway. *J. Struct. Geol.*, **10**, 1385–1401.
- Roberts, D., 1983. Devonian tectonic deformation in the Norwegian Caledonides and its regional perspectives. *Nor. Geol. U. Bull.*, **380**, 85–96.
- Sibson, R.H., 1977. Fault rocks and fault mechanisms. *J. Geol. Soc. London*, **133**, 191–213.
- Smith, D.C., 1984. Coesite in clinopyroxene in the Caledonides and its implications for geodynamics. *Nature*, **310**, 641–644.
- Torsvik, T.H., Andersen, T.B. and Van Eide, E.A., 1997. The age and tectonic significance of dolerite dykes in Western Norway. *J. Geol. Soc. London*, in press.
- Torsvik, T.H., Smethurst, M.A., Meert, J.G., Van der Voo, R., McKerrow, W.S., Brasier, M.D., Sturt, B.A. and Walderhaug, H.J., 1996. Continental break-up and collision in the Neoproterozoic and Palaeozoic—A tale of Baltica and Laurentia. *Earth Sci. Rev.*, **40**, 229–258.
- Torsvik, T.H., Sturt, B.A., Swenson, E., Andersen, T.B. and Dewey, J.F., 1992. Palaeomagnetic dating of fault rocks: evidence for Permian and Mesozoic movements and brittle deformation along the extensional Dalsfjord Fault, western Norway. *Geophys. J. Int.*, **109**, 565–580.
- Van der Voo, R., 1993. *Paleomagnetism of the Atlantic, Tethys and Iapetus Oceans*. Cambridge University Press, New York.
- Wise, D.U., Dunn, D.E., Engelder, J.T., Geiser, P.A., Hatcher, R.D., Kish, S.A., Odom, A.L. and Schamel, S., 1984. Fault-related rocks: Suggestions for terminology. *Geology*, **12**, 391–394.

Received 9 April 1997; revised version accepted 19 September 1997